The Role of Hydrogen Bond Acceptor Groups in the Interaction of Substrates with Pdr5p, a Major Yeast Drug Transporter†

Leanne Hanson,‡ Leopold May,§ Pamela Tuma,‡ James Keeven,‡ Patrick Mehl,|| Michelle Ferenz,⊥ Suresh V. Ambudkar,# and John Golin*,‡

Departments of Biology and Chemistry and The Vitreous State Laboratory, The Catholic University of America, Washington, D.C. 20064, Department of Biology, Dickinson College, Carlisle, Pennsylvania 17013, and Laboratory of Cell Biology, Center for Cancer Research, National Cancer Institute, National Institutes of Health, Bethesda, Maryland 20892-4256

Received February 18, 2005; Revised Manuscript Received May 10, 2005

ABSTRACT: The yeast ABC (ATP-binding cassette protein) multidrug transporter Pdr5p transports a broad spectrum of xenobiotic compounds, including antifungal and antitumor agents. Previously, we demonstrated that substrate size is an important factor in substrate−transporter interaction and that Pdr5p has at least three substrate-binding sites. In this study, we use a combination of whole cell transport assays and photoaffinity labeling of Pdr5p with [^{125}I]iodoarylazidoprazosin in purified plasma membrane vesicles to study the behavior of two series of novel substrates: trityl (triphenylmethyl) and carbazole derivatives. The results indicate that site 2, defined initially by tritylimidazole efflux, requires at least a single hydrogen bond acceptor group (electron pair donor). In contrast, complete inhibition of rhodamine 6G efflux and [^{125}I]iodoarylazidoprazosin binding at site 1 requires substrates with three electronegative groups. Carbazole and trityl substrates with two groups show saturating, incomplete inhibition at this site. This type of inhibition is frequently observed in bacterial multidrug-binding proteins that use a pocket with multiple binding sites. The presence of multiple sites with different requirements for substrate−Pdr5p interaction may explain the broad specificity of xenobiotic compounds transported by this protein.

The yeast *PDR5* locus encodes a 160 kDa member of the ATP-binding cassette (ABC)[1] superfamily of transporters, and it transports a broad array of mechanistically and structurally distinct xenobiotic compounds (*1*−*4*). Although multidrug transporters are ubiquitous and of great clinical relevance, relatively little is known about their substrate specificity. Such knowledge is potentially important for the design of antifungal and antitumor agents or inhibitors of transporter activity. Recent work in our laboratories with several series of structurally related compounds demonstrated that substrate size is of critical importance in the interaction with Pdr5p (*5*). Transport is most efficacious with xenobiotic compounds of ∼200 Å^3, whereas compounds with surface volumes less than ∼90 Å^3 are extremely poor substrates. In contrast to the somewhat narrow size range for optimal substrates, Pdr5p substrates show a broad range of log *P* values and thus vary greatly in their relative hydrophobicity.

Our studies also demonstrated that at least three sites are involved in substrate−transporter interaction. It is not clear, however, how these sites are arranged. For instance, by analogy to the *Escherichia coli ACR*B and *Staphylococcus aureus QACR*-encoded multidrug-binding proteins, which have been crystallized with their ligands (*6*, *7*), there could be a large binding pocket with multiple domains capable of binding more than one substrate at a time. Alternatively, we cannot exclude the possibility that Pdr5p has three spatially distinct sites.

Of primary importance is an understanding of the arrangement and chemical specificity of the Pdr5p substrate-binding sites, properties that remain unclear for virtually all eukaryotic multidrug transporters. We used a series of relatively simple trityl and carbazole derivatives to explore the chemical specificity of two Pdr5p binding sites that exhibit different substrate specificities. This approach is a novel one; to date it has been applied only to Pdr5p. Site 1 is used for efflux of substrates such as rhodamine 6G and the clinically important antifungal agent clotrimazole. Our data support two possible models for the arrangement of electronegative groups. One model requires that substrates have at least three hydrogen bond acceptor groups (electron pair donors). The second model requires two electron pair donors and a third electronegative group on an aromatic ring that promotes electrostatic interactions between a substrate and site 1. The distances between the electronegative groups may also be important. We also demonstrate that site 1 is specifically cross-linked by the prazosin derivative iodoarylazidoprazosin (IAAP). Site 2, which is responsible for the efflux of

† This work was supported by a grant-in-aid from The Catholic University of America to J.G. and a Howard Hughes Undergraduate Research Award to M.F.

* Corresponding author: 202-319-5722 (phone); 202-319-5721 (fax); golin@cua.edu (e-mail).

‡ Department of Biology, The Catholic University of America.

§ Department of Chemistry, The Catholic University of America.

|| The Vitreous State Laboratory, The Catholic University of America.

⊥ Department of Biology, Dickinson College.

Laboratory of Cell Biology, Center for Cancer Research, NCI.

[1] Abbreviations: ABC, ATP-binding cassette; MIC, minimum inhibitory concentration; trityl, triphenylmethyl; IAAP, iodoarylazidoprazosin; FACS, fluorescence-activated cell sorting; UTPase, uridine-triphosphatase; ITEA, 2-(1*H*-indol-3-yl)-*N*-tritylethanamine; ellipticine, 5,11-dimethyl-6*H*-pyrido[4,3-*b*]carbazole; NCC, 9-[*N*-(4-chlorophenyl)carbamoyl]carbazole; Δ, deletion.

10.1021/bi0502994 CCC: $30.25
Published on Web 06/18/2005

tritylimidazole, requires a single hydrogen bond acceptor group.

EXPERIMENTAL PROCEDURES

Yeast Strains and Media. The yeast strains used in this study, AD124567 and AD1−7, were previously described (*8*). AD124567 overexpresses Pdr5p and is otherwise isogenic to AD1−7, which lacks all of the ABC multidrug transporters. The latter carries a substantial deletion of *PDR5*. For transport studies and minimum inhibitory concentration (MIC) determination, strains were cultured in SD complete medium (per liter: 20 g of glucose, 7.5 g of yeast nitrogen base, 0.0005% added amino acids, adenine, and uracil) until reaching a concentration of (∼2−4) × 10^7 cells/mL. To produce cells for membrane vesicle preparation, the strains were grown in YPD medium (per liter: 20 g of glucose, 20 g of peptone, and 10 g of yeast extract). Growth of cultures was monitored with a Spectronic 20D+ spectrophotometer (Milton Roy, Ivyland, PA).

Chemicals. All nonradioactive chemicals were purchased from Sigma-Aldrich (St. Louis, MO) except for tripentyltin chloride, which was obtained from Organometallics Inc. (East Hampstead, NH). [^{3}H]Tritylimidazole (25 Ci/mmol) and [^{125}I]IAAP (2200 Ci/mmol) were obtained from American Radiolabeled Chemicals (St. Louis, MO) and PerkinElmer Life Sciences (Boston, MA), respectively. Nonradioactive substrates were dissolved in DMSO.

Transport Assays. [^{3}H]Tritylimidazole efflux was monitored as previously described (*5*). Transport of rhodamine 6G was carried out with a fluorescence-activated cell-sorting (FACS) assay modified slightly from that of Kolaczkowski et al. (*2*). Ten milliliter cultures of exponentially growing yeast cells were washed twice with sterile reverse-osmosis water and once with 0.05 M Hepes buffer (pH 7.0) before resuspension in Hepes buffer and determination of the cell concentration. In each assay, 10^6 cells were pelleted in Eppendorf tubes and resuspended in 400 μL of Hepes buffer containing 1.25, 2.5, or 5.0 μM rhodamine 6G and any substrates being studied. Cells were incubated at 30 °C for 2 h. Following loading, they were pelleted, washed once in Hepes buffer, and resuspended in 400 μL of Hepes (pH 7.0) plus 1 mM glucose with or without substrate. Following incubation for 30 min at 30 °C, cells were placed on ice for 5 min. They were washed once with cold Hepes buffer before being resuspended in 300 μL of Hepes buffer. Rhodamine 6G fluorescence was measured with a Becton-Dickinson FACSort with an excitation wavelength of 488 nm and an emission wavelength of 585 nm. The data were analyzed with a CellQuest program. Retained fluorescence is expressed in arbitrary units.

Preparation of Purified Plasma Membrane Vesicles. The procedure for the preparation of yeast plasma membrane vesicles was recently described (*9*), except for two modifications. Instead of lysing yeast cells manually with glass beads, we used a Bead-Beater (Biospec Products, Bartlesville, OK). Up to 2 L of exponentially growing cells was used for each preparation. Seven protease inhibitors were present continuously during and after breakage: 1 mM phenylmethanesulfonyl fluoride; 2.5 mM EDTA; 1 μg/mL leupeptin, pepstatin A, and aprotinin; and 10 μg/mL TPCK and TLCK. Phenylmethanesulfonyl fluoride (1 mM) was also added to the culture medium just before harvesting.

Determination of Protein Concentration. The protein concentration of the purified vesicles was determined with a bicinchoninic acid kit (Perbio, Rockland, IL).

Uridinetriphosphatase Assay. The quality of Pdr5p in the membrane preparations was assayed by taking advantage of its unique uridinetriphosphatase (UTPase) activity. This assay was previously described (*9*). Each assay was carried out with 30 μg of plasma membrane vesicle protein.

Photoaffinity Labeling of Pdr5p with [^{125}I]IAAP. Photoaffinity labeling was carried out by slightly modifying the procedure described for mammalian transporters (*10*). Purified plasma membrane vesicle protein (30 μg) was used in each sample. Samples were incubated with competing substrates for 5 min at room temperature before 5−10 nM [^{125}I]IAAP was added. Samples were incubated for an additional 10 min, after which time they were cross-linked for 10 min with 365 nm UV light. After cross-linking, the vesicles were solubilized in SDS−PAGE. Gel electrophoresis was performed with 7% NuPAGE gels (InVitrogen, Carlsbad, CA) at constant voltage (15 min at 50 V, then 175 V until the dye front ran off the gel). Following electrophoresis, gels were stained with Collodial Blue and dried. The radioactivity incorporated into the Pdr5p band was quantified with a STORM 860 phosphorimager system (Molecular Dynamics, Inc., Sunnyvale, CA) and ImageQuant software.

Calculation of Molecular Size Parameters. The software to determine the surface volume of Pdr5p substrates and the distances between electronegative groups was previously described (*5*). The shortest distance between groups in the most stable configuration was determined. An improved version, CACHE 5.0, was used in these calculations.

Determination of MICs. MICs were determined on solid medium as previously described (*5*). The first MIC ratio for each substrate was determined with the wild-type strain (RW2802, *PDR5*) and the isogenic mutant strain (JG436, *pdr5:Tn5*). These were the original strains used to study Pdr5p function (*11*, *12*) and substrate specificity (*4*).

A second MIC ratio was also obtained with the strains used in this study: AD124567 (*PDR5*) and AD1−7 (*pdr5*Δ). The high-level resistance found in the AD124567-overproducing strain makes it impossible to find the MIC for most of these substrates. Thus, the last soluble concentration is used in the calculation of the ratio and a ≥ designation is employed.

RESULTS

Use of Trityl and Carbazole Derivatives as Pdr5p Substrates. The structures of the substrates used to study two Pdr5p binding sites are found in Figure 1 along with distances between electronegative groups. Surface volumes and MIC ratios are listed in Table 1. We observed previously, through a MIC assay, that tritylimidazole (Figure 1B) and clotrimazole (Figure 1C) are equally potent Pdr5p substrates (*5*). A strain missing Pdr5p function is ∼300-fold more sensitive than the isogenic Pdr5p strain to each of these compounds. The only difference between the two substrates is a chlorine atom on one of the phenyl groups. Nevertheless, there is a large difference in their ability to inhibit [^{3}H]chloramphenicol efflux from whole cells. This suggested the existence of multiple sites for transporter−substrate interaction and the possibility that site selection is governed

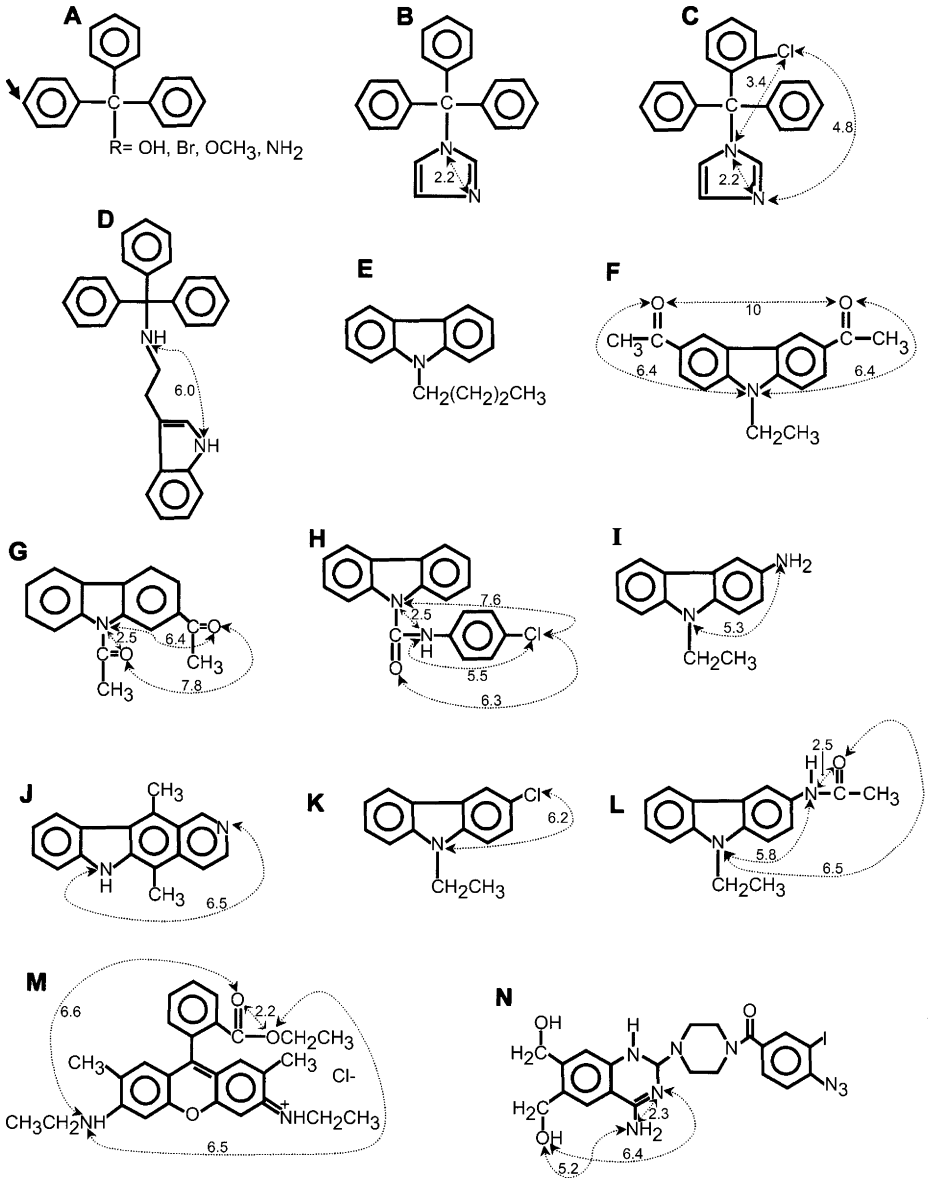

FIGURE 1: Structures of substrates. (A) Trityl derivatives where R = Br, NH_2OCH_3, or OH. The arrowhead points to the location of the ether group in 4-methoxytrityl. (B) Tritylimidazole. (C) Clotrimazole. (D) ITEA. (E) 9-Butylcarbazole. (F) 3,6-Diacetyl-9-ethylcarbazole. (G) 2,9-Diacetylcarbazole. (H) NCC. (I) 3-Amino-9-ethylcarbazole. (J) Ellipticine. (K) 3-Chloro-9-ethylcarbazole. (L) 3-Acetoamido-9-ethylcarbazole. (M) Rhodamine 6G. (N) IAAP. Dashed lines indicate the distances (Å) between electronegative groups. Because NCC, rhodamine, and IAAP have more than three electronegative groups, only a few of the distances are indicated.

in part by the number and/or spacing of electronegative groups. To investigate the role of these groups in Pdr5p−substrate interactions, we used several additional trityl derivatives (Figure 1B−D) as well as a series of substituted carbazoles (Figure 1E−L).

Although the two series studied contain aromatic groups, their structures are otherwise quite different. The carbazoles are planar molecules, and the trityl derivatives are globular or nonplanar. The compounds differ in the number and strength of the electronegative groups. Clotrimazole (Figure 1C), both diacetylcarbazole derivatives (Figure 1F,G), and 3-acetoamido-9-ethylcarbazole (Figure 1L) have three such groups. Substrates with two groups include tritylimidazole (Figure 1B), 2-(1*H*-indol-3-yl)-*N*-tritylethanamine (ITEA; Figure 1D), 3-amino-9-ethylcarbazole (Figure 1I), 5,11-dimethyl-6*H*-pyrido[4,3-*b*]carbazole (ellipticine; Figure 1J), and 3-chloro-9-ethylcarbazole (Figure 1K). In the last four, the distance between the two nitrogens is much greater (6.0, 5.3, 6.2, and 6.5 Å) than in tritylimidazole (2.3 Å) and much like those observed in clotrimazole and rhodamine 6G. Of the remaining carbazole derivatives used in this study, 9-butylcarbazole (Figure 1E) has one electronegative group. Finally, 9-[*N*-(4-chlorophenyl)carbamoyl]carbazole (NCC; Figure 1H) has four electronegative groups with distances between them that are similar to 2,9-diacetylcarbazole and rhodamine 6G (Figure 1M). Not all of the compounds are toxic to our yeast strains. In those cases, a MIC ratio cannot be determined. The ratios for most carbazole derivatives are similar (Table 1).

Trityl Derivatives with Only One Hydrogen Bond Acceptor Group Inhibit [^{3}H]Tritylimidazole Efflux. Our previous work (*5*) demonstrated that trialkyltin chlorides do not inhibit chloramphenicol (site 1) transport. Instead, these substrates are effective inhibitors of tritylimidazole (site 2) efflux. In contrast, tetrapropyltin fails to inhibit either substrate (*5*). This suggests that only one hydrogen bond acceptor group

Table 1: Molecular Size and Substrate Efficacy

compound[a]	surface volume (Å^3)	MIC ratios[b]
tritylamine	172.70	
trityl bromide	199.04	
trityl ether	194.35	
4-methoxytrityl	199.64	
tritylmethanol	199.04	
tritylimidazole	200.33	320, ≥800
clotrimazole	208.36	320, ≥1000
ITEA	261.10	
9-butylcarbazole	153.16	
3,6-diacetyl-9-ethylcarbazole	179.10	16, ≥32
2,9-diacetylcarbazole	177.16	8, ≥8
3-amino-9-ethylcarbazole	142.25	
ellipticine	160.59	8, ≥8
3-chloro-9-ethylcarbazole	142.25	2.5, ≥4
NCC	182.53	8, ≥16
3-acetoamido-9-ethylcarbazole	147.66	2, 4
rhodamine 6G	285.87	50, ≥100
IAAP	261.83	

[a] Substrates are listed in the same order as found in Figure 1. [b] Two ratios are given for each compound where MICs can be determined. The first ratio is derived from the isogenic strains RW2802 (*PDR5*) and JG436 (*pdr5::Tn5*). Pdr5p is not overexpressed in the former and is not transcribed in the latter (*1*). These strains were used to initially study Pdr5p−substrate specificity (*4*). The second ratio was obtained from the isogenic pair of strains (AD1−7, AD124567) used in this study. See the Experimental Procedures for additional details.

is sufficient for site 2, provided other criteria, such as size, are met. To examine this possibility, we compared carbazole and trityl derivatives containing a single potential hydrogen bond acceptor for the ability to inhibit [^{3}H]tritylimidazole efflux. The data from the trityl derivatives are presented in Figure 2A−C. Each panel in the figure represents a separate experiment. Although the cultures were grown under similar conditions, the variation in the amount of tritylimidazole retained in the untreated, control strains was as much as 2-fold over the course of several months of experimentation. Therefore, inhibition of tritylimidazole efflux is considered complete when the level of retained [^{3}H]tritylimidazole in the treated sample is the same as that observed in the *pdr5*Δ control strain from the same experiment. The value for the latter is indicated on the *y*-axis of each figure.

We also tested the amount of retained [^{3}H]tritylimidazole in the *pdr5*Δ strain in the presence of the highest concentration of competing substrate to determine whether any retention was Pdr5p independent. Figure 2A compares tritylmethanol, trityl ether, and trityl bromide. In contrast to the other groups, only the alcohol shows concentration-dependent inhibition of [^{3}H]tritylimidazole efflux with an I_{50} that is ∼40 μM. Trityl bromide and trityl ether significantly increase the amount of retained [^{3}H]tritylimidazole ∼1.5-fold relative to the Pdr5p control, but the inhibition is incomplete and concentration independent. A similar result was observed with 4-methoxytrityl (Figure 2B). Finally, we demonstrated similar inhibition with tritylamine and tritylmethanol (Figure 2C).

We also tested the ability of 9-butylcarbazole to inhibit efflux. These results are found in Figure 2D, where two independent experiments are compared. The inhibition is concentration dependent but weak, with an I_{50} of ∼100 μM. Addition of 200 μM competing substrate to *pdr5*Δ in experiment 1 yielded 13 ± 2.5 pM [^{3}H]tritylimidazole/10^7 cells. This does not represent a significant increase when compared to the untreated *pdr5*Δ control (12 ± 2 pM [^{3}H]tritylimidazole/10^7 cells). Therefore, the observed concentration-dependent inhibition is attributable to Pdr5p.

Trityl substrates with an amino or an alcohol group and a carbazole with an aromatic tertiary amine show concentration-dependent inhibition. Trityl derivatives with an ether, methoxy, or bromine group do not.

Effect of Trityl Derivatives on Rhodamine 6G Efflux. Unlike tritylimidazole, clotrimazole causes complete, concentration-dependent inhibition of chloramphenicol efflux (*5*). This observation suggested several models for site 1 substrate requirements. The first is that all of the electronegative groups serve as electron pair donors. Thus, in this model, the chlorine atom is a weak hydrogen bond acceptor, and the difference between clotrimazole and tritylimidazole behavior is in the number and/or arrangement of such groups. Tritylimidazole is ineffective because either three hydrogen bond acceptor groups are required or two groups are sufficient but must be farther apart than the two nitrogens in the imidazole ring.

The second model posits both electron pair donors and electrostatic interaction between an aromatic group and Pdr5p. In this model, the nitrogen atoms form hydrogen bonds, but the chlorine atom alters the capability of the phenyl group to interact electrostatically and thus facilitates binding at site 1. To explore these possibilities, we made use of a rhodamine 6G transport assay. Rhodamine 6G (Figure 1M) transport was shown to be competitively inhibited by chloramphenicol (*2*). Conversely, rhodamine 6G completely inhibits chloramphenicol efflux. Following the previously published chloramphenicol transport assay (*5*), we observed complete inhibition of efflux with 25 μM rhodamine 6G. Thus, rhodamine 6G is a site 1 substrate. We initially verified that rhodamine efflux is blocked by the addition of 2-deoxyglucose and is therefore energy dependent (data not shown).

The results with the trityl compounds are found in Figure 3. Figure 3A is a control experiment demonstrating that the *pdr5*Δ mutant strain has an ∼150-fold greater retained fluorescence than its isogenic Pdr5p-overproducing counterpart. In 12 experiments and 24 determinations with 5.0 μM rhodamine 6G, the median fluorescence retained in the Pdr5p ranged from 4.61 to 125 (median value = 12.0) and from 1140 to 2100 (median value = 1470) in the *pdr5*Δ strain. Because of this variation, we measured retained fluorescence in the *pdr5*Δ control in every experiment. A competing substrate is said to show complete inhibition when it reaches this level or approaches it closely. There is always a large difference between the two strains (median difference is ∼120-fold). As shown in Figure 3B, clotrimazole exhibits concentration-dependent inhibition of rhodamine efflux. The I_{50} is ∼30 μM. Addition of 25 μM gave a median retained fluorescence of 429, and complete inhibition was obtained with 40 μM (1300; 1330 was observed in the untreated *pdr5*Δ and 9.47 in the *PDR5* strain). The tritylimidazole FACS histogram plots (Figure 3C) from the same experiment as the clotrimazole data demonstrate that there is little or no inhibition with concentrations up to 25 μM.

ITEA (Figure 1D) has two putative hydrogen bond acceptor groups separated by a distance that is between those found in clotrimazole and those observed in rhodamine 6G, yet it fails to show complete, concentration-dependent

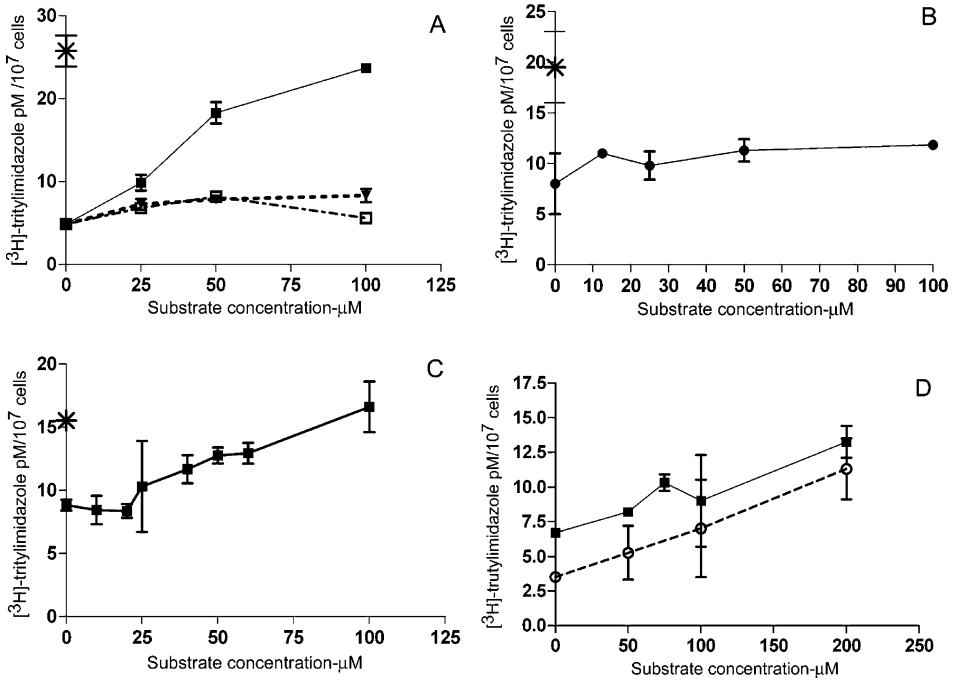

FIGURE 2: Inhibition of [^{3}H]tritylimidazole efflux as a function of substrate concentration. (A) Tritylmethanol (■) has an I_{50} of ∼40 μM; trityl bromide (■) and ether (▼) do not show concentration-dependent inhibition. In this experiment, the untreated *pdr5*Δ and *PDR5* strains retained 28 pM/10^7 cells and 4.8 ± 0.6 pM/10^7 cells, respectively. (B) The effect of 4-methoxytrityl (●) is weak and does not show concentration dependence. Although the value of 12 ± 0.2 pM/10^7 cells reached at 100 μM is higher than the control (8.0 ± 3.0 pM/10^7 cells), it is well below the value observed in the *pdr5*Δ control (20 ± 3.5 pM/10^7 cells). (C) Tritylamine (■) exhibits an inhibition pattern similar to tritylmethanol. At 100 μM, the value of 16 ± 2.7 pM/10^7 cells is the same as the *pdr5*Δ strain (16 ± 2.7 pM/10^7). (D) 9-Butylcarbazole shows weak, concentration-dependent inhibition. Data from two independent experiments are shown. The *pdr5*Δ was not run in experiment 2 (○). For panels A−C, the amount of [^{3}H]tritylimidazole retained by the untreated *pdr5*Δ strain is indicated by a symbol (*) on the *y*-axis. In experiment 1 (■), this strain retained 13 ± 2.5 pM [^{3}H]tritylimidazole/10^7 cells.

inhibition at site 1 over a range of concentrations up to 50 μM (data not shown). Figure 3D compares the effect of 40 μM clotrimazole, tritylimidazole, and ITEA on rhodamine efflux. ITEA causes somewhat greater retention of fluorescence than does tritylimidazole (median fluorescence: 112, compared with 34.2) and the control (12.8), but only clotrimazole approaches complete inhibition (1340, compared with 2099 for the *pdr5*Δ). ITEA, however, inhibits [^{3}H]-tritylimidazole efflux. Thus, the substrate enters the cell and interacts with Pdr5p (data not shown). These results suggest that two electron pair donor groups are insufficient for inhibition of rhodamine 6G and indicate that interaction at site 1 has an additional requirement. Carbazole derivatives were used to extend these studies.

2,9-Diacetylcarbazole and NCC Show Significant Concentration-Dependent Inhibition of Rhodamine 6G Efflux. The data in Table 1 demonstrate that many of the carbazole derivatives have approximately the same volume and produce similar MIC ratios. This suggests that these derivatives are of nearly the same strength as Pdr5p substrates. Three carbazole derivatives in our study have three electronegative groups: 3,6-diacetyl-9-ethylcarbazole (Figure 1F), 2,9-diacetylcarbazole (Figure 1G), and 3-acetoamido-9-ethylcarbazole (Figure 1L). Of particular note is that the distances between the groups in 3,6-diacetyl-9-ethylcarbazole are 6.4 Å, 6.4 Å (N−O), and 10 Å (O−O). The absence of two groups a short distance apart is significant. In contrast, 2,9-diacetylcarbazole has distances of 6.4, 7.8, and 2.5 Å, which are similar to those found in rhodamine 6G (2.2, 6.5, and 6.6 Å). Similarly, the distances between groups in 3-acetoamido-9-ethylcarbazole are 6.4, 5.6, and 2.5 Å. On the basis of this information, we predicted that 2,9-diacetylcarbazole would be a better inhibitor of rhodamine 6G efflux than 3,6-diacetyl-9-ethylcarbazole.

The data in Figure 4A show the effect of 2,9-diacetylcarbazole on the efflux of 1.25, 2.5, and 5.0 μM rhodamine 6G. In addition, the effect of 3,6-diacetyl-9-ethylcarbazole concentration on the efflux of 5.0 μM rhodamine is also shown. Concentration-dependent inhibition is observed for both 2,9-diacetylcarbazole and 3,6-diacetyl-9-ethylcarbazole. With respect to the former, a plot of rhodamine 6G concentration versus I_{50} is linear. The I_{50} values for the three concentrations of rhodamine are ∼9, 20, and 40 μM. Thus, 2,9-diacetylcarbazole has the features of a competitive inhibitor. The effect of 3,6-diacetyl-9-ethylcarbazole on inhibition is much weaker. Histogram plots comparing the effect of 100 μM on the inhibition of 5.0 μM rhodamine 6G efflux are found in Figures 4B (3,6-diacetyl-9-ethylcarbazole), 4C (2,9-diacetylcarbazole), and 4D (Pdr5p, no substrate control). While ∼30% of cells show complete inhibition of efflux with 3,6-diacetyl-9-ethylcarbazole, the remainder exhibit a broad range of retained fluorescence that represents loss of rhodamine (Figure 4B). In contrast, the profile of 2,9-diacetylcarbazole is much like that observed with the *pdr5*Δ mutant (Figure 4C). Lowering the concentration of rhodamine to 1.5 μM does not increase the proportion of cells showing complete inhibition (J. Golin, unpublished observations).

In an additional experiment, we added 150 μM 2,9-diacetylcarbazole to the *pdr5*Δ control strain (AD1−7) to determine whether the substrate increases the amount of fluorescence in the absence of the transporter. The mean

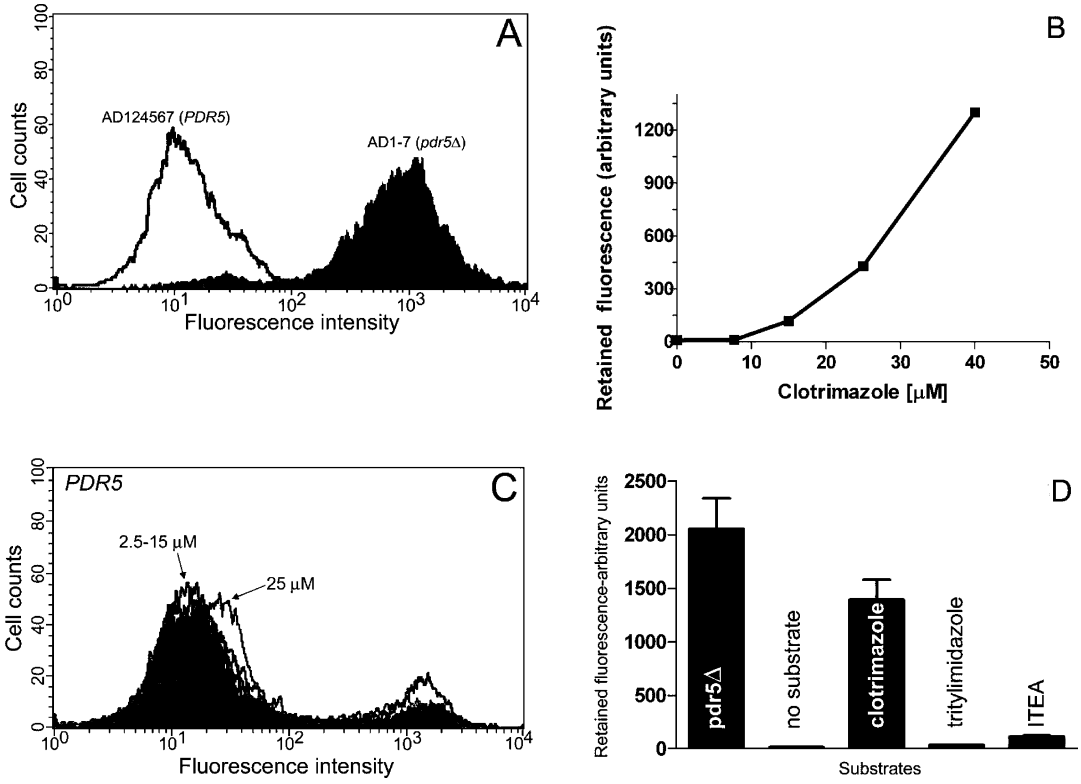

FIGURE 3: Inhibition of rhodamine 6G efflux by trityl derivatives. (A) Rhodamine 6G accumulation histogram plot of isogenic *pdr5*Δ and *PDR5* strains showing an ~150-fold differential in retained fluorescence. (B) Concentration-dependent inhibition of rhodamine 6G by clotrimazole. 10^6 cells were preloaded with 5.0 μM rhodamine 6G. Following this, they were resuspended for 30 min in buffer without rhodamine in the presence or absence of competing substrate. Retained fluorescence was determined by FACS as described in the Experimental Procedures. The median values from a representative experiment indicate an I_{50} of ~30 μM. (C) Histogram plot of tritylimidazole showing little or no inhibition of rhodamine efflux at concentrations up to 25 μM. (D) Comparison of cells with no competing substrate (NS), clotrimazole (CLO), tritylimidazole (TRIT), and ITEA. The amount of competing substrates added was 40 μM. The median retained fluorescence in this experiment was 2100 for AD1−7 and 13.10 for AD124567.

values obtained with 2,9-diacetylcarbazole were less than with the *pdr5*Δ strain incubated in the absence of this substrate (1780 ± 13 in the former, 1940 ± 9.0 in the latter). This might explain why 100 μM reaches a level much like that observed in the *pdr5*Δ control, while cells at the highest concentration tested (200 μM) show a small decrease in retained fluorescence in the Pdr5p strain (data are not shown, but the median retained fluorescence is 1200 arbitrary units).

NCC (Figure 1H) has four electronegative groups with distances much like those found in rhodamine 6G and 2,9-diacetylcarbazole. Figure 5 contains data indicating that NCC effectively inhibits efflux. At 100 μM, the NCC and 2,9-diacetylcarbazole peaks coincide and are of similar area, indicating that rhodamine 6G efflux is inhibited in most of the cells with both substrates (the median fluorescence for the AD1−7 control is similar to 2,9-diacetylcarbazole). Nevertheless, a small proportion of cells (~20%) show reduced fluorescence with NCC that is absent at higher 2,9-diacetylcarbazole concentrations.

The carbazole derivatives showing complete inhibition of site 1 contain three electronegative groups. According to the first model, all of these are regarded as electron pair donors. According to the second model, the electronegative atoms attached to the aromatic rings change their electrostatic properties and promote substrate−site 1 interaction. In all of the substrates examined thus far, these groups are ring deactivators (electron-withdrawing groups resulting in a ring with increased positive charge).

Carbazole Derivatives with Two Electronegative Groups Exhibit Saturating, Incomplete Inhibition. We also examined the effect of 3-amino-9-ethylcarbazole (Figure 1I), ellipticine (Figure 1J), and 3-chloro-9-ethylcarbazole (Figure 1K) on efflux. All have two electronegative groups that are ~5−7 Å apart. Their individual effects on the phenyl group are different. The chlorine group on 3-chloro-9-ethylcarbazole is a ring deactivator (electron-withdrawing group), while 3-amino-9-ethylcarbazole contains an activator group (electron-contributing group). Ellipticine has two amines that are part of aromatic rings and might serve as electron pair donors. All three behave similarly and show saturating incomplete inhibition.

One set of amino derivative samples was analyzed. They do not vary significantly over a range of 50−200 μM and show the weakest inhibition, with a maximum retained fluorescence only 1.7 times that of the untreated Pdr5p strain and 0.16 times that of the *pdr5*Δ control strain. The chlorocarbazole derivative reached 0.25 ± 0.08 of the retained fluorescence found in the *pdr5*Δ strain. Figure 6 shows the effect of varying the ellipticine concentration on efflux (the profile of 25 μM 2,9-diacetylcarbazole from the same experiment is provided for comparison). There is little concentration dependence, and the inhibition is incomplete. This behavior (as well as that observed with the chloro and amino derivatives), however, differs from that of 3,6-diacetyl-9-ethylcarbazole. In the latter, a significant proportion of the cells exhibit complete inhibition of rhodamine 6G efflux.

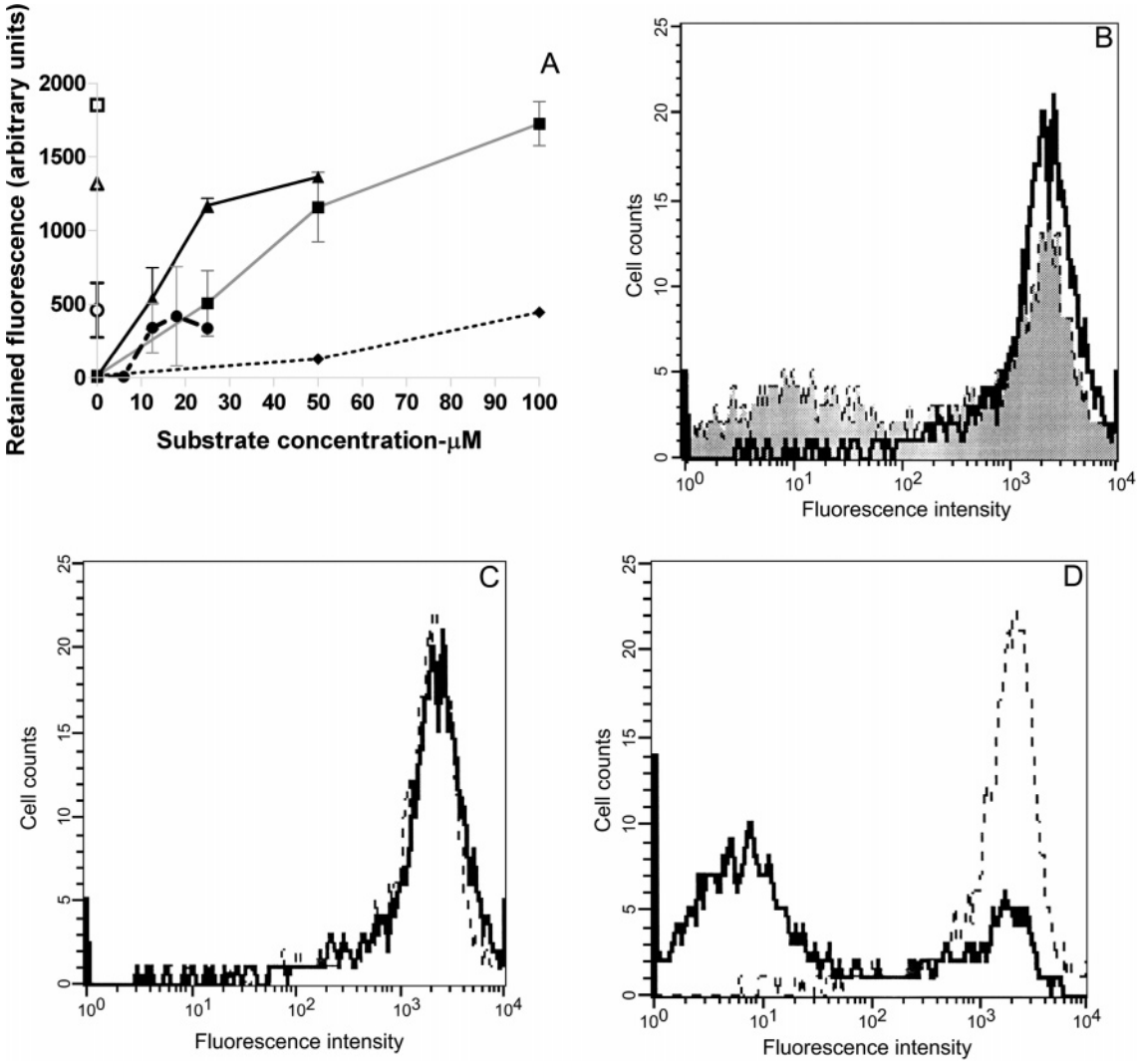

FIGURE 4: Concentration-dependent inhibition of rhodamine 6G by 2,9-diacetylcarbazole and 3,6-diacetyl-9-ethyl chloride. (A) 2,9-Diacetylcarbazole shows strong concentration-dependent inhibition of rhodamine 6G efflux. The plots show the effect of varying 2,9-diacetylcarbazole concentration on 1.25, 2.5, and 5.0 μM rhodamine 6G efflux. Also shown is the effect of 3,6-diacetyl-9-ethylcarbazole on the efflux of 5.0 μM rhodamine 6G. All of the FACS experiments in this paper were performed with duplicate samples, but only one sample is shown in the histogram plots for simplicity. The other member of each pair gave similar results. Key: (■) 5.0 μM rhodamine 6G; (▲) 2.5 μM rhodamine 6G; (●) 1.25 μM rhodamine 6G; (◆) 3,6-diacetyl-9-ethylcarbazole plus 5.0 μM rhodamine 6G; (□) pdr5Δ−5.0 μM rhodamine; (△) pdr5Δ−2.5 μM rhodamine; (○) pdr5Δ−1.25 μM rhodamine. (B) Although 3,6-diacetyl-9-ethylcarbazole has a high proportion of cells showing significant efflux of rhodamine 6G, the peak representing maximum fluorescence completely overlaps that of 2,9-diacetylcarbazole and the *pdr5*Δ control, suggesting that 3,6-diacetyl-9-ethylcarbazole is acting weakly at site 1, causing complete inhibition in about 30% of the cells. (C) The peak of retained fluorescence observed with 100 μM 2,9-diacetylcarbazole (—) and that observed with the *pdr5*Δ (- - -) control are nearly identical. (D) Control histogram plots of AD1−7 (- - -) and AD124567 (—) showing retained fluorescence in the absence of competing substrates.

The results with two group carbazole derivatives are therefore similar to those found with ITEA (Figure 1D).

Behavior of 3-Acetoamido-9-ethylcarbazole. The Pdr5p substrate 3-acetoamido-9-ethylcarbazole (Figure 1L) also has three electronegative groups with the requisite distances; however, the acetoamido derivative is a ring activator rather than a ring deactivator. The ability of 3-acetoamido-9-ethylcarbazole to inhibit rhodamine 6G transport was tested along with 2,9-diacetylcarbazole and 3,6-diacetyl-9-ethylcarbazole. The results are found in Figure 7, which shows representative histogram plots. Although the two diacetyl derivatives continued to behave as described above, 3-acetoamido-9-ethylcarbazole showed no inhibition when 50, 100, and 150 μM concentrations of this substrate were tested. In contrast, when this compound was tested in the [^{3}H]tritylimidazole transport assay, the I_{50} was ~60 μM.

[^{125}I]IAAP Cross-Links Pdr5p Binding Site 1. The prazosin derivative IAAP is capable of specifically cross-linking Cdr1p and P-glycoprotein, two well-characterized multidrug transporters (*9*, *10*). This reagent therefore facilitates a direct look at the binding capability of different substrates. For this reason, the interaction of Pdr5p with this compound was tested for the first time. Its chemical structure (Figure 1N) indicates that IAAP should interact at the same binding site as rhodamine 6G, because both have the requisite number of electronegative groups. As shown below, this is the case. Because comparisons of tritylimidazole and clotrimazole transport in inhibition assays of either rhodamine or chloramphenicol efflux indicate a marked difference, we sought to determine whether this behavior was also observed when the imidazole derivatives were used in competition experiments with [^{125}I]IAAP. These data are found in Figure 8.

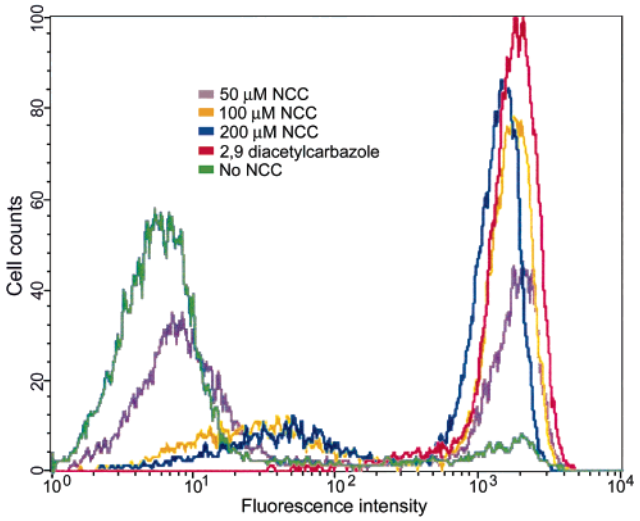

FIGURE 5: Concentration-dependent inhibition of rhodamine efflux by NCC. Histogram plots of retained rhodamine 6G fluorescence in the presence of NCC (0, 50, 100, and 200 μM) demonstrate concentration-dependent, nearly complete inhibition of rhodamine efflux. In these experiments, 5.0 μM rhodamine 6G was used. The *pdr5*Δ control had a median retained fluorescence of 1940 ± 14; the Pdr5p samples containing 50 μM 2,9-diacetylcarbazole had a value of 1779 ± 51.

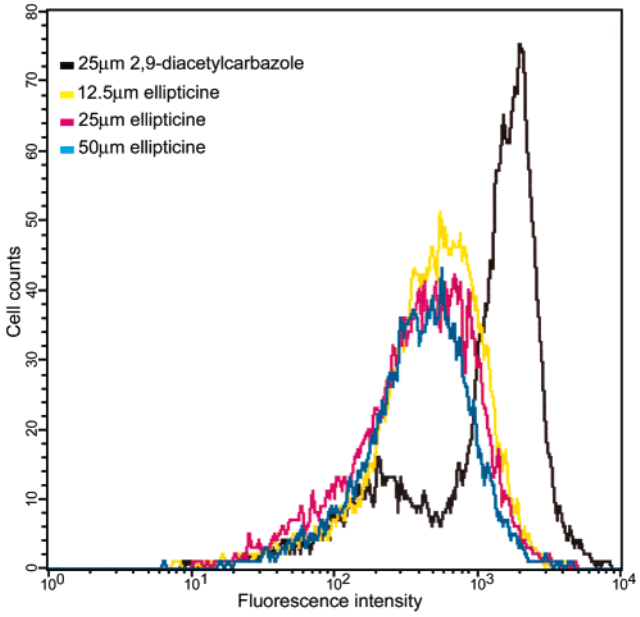

FIGURE 6: Saturating, incomplete inhibition by ellipticine, a carbazole derivative with two electronegative groups. The rhodamine 6G transport assay is the same as that described above. Histogram plots showing incomplete, saturating inhibition of 2.5 μM rhodamine efflux by ellipticine (12.5, 25, and 50 μM). The profile of 25 μM 2,9-diacetylcarbazole is provided for comparison.

Figure 8A shows that a plasma membrane vesicle preparation from the Pdr5p strain produces an abundant 160 kDa band that is missing from the isogenic *pdr5*Δ mutant. This preparation was used for most of the cross-linking studies. On average, it had a Pdr5p-specific UTPase activity of 0.3 mmol mg^{-1} min^{-1} that is 4-fold greater than the activity caused by background spontaneous hydrolysis of UTP in the absence of vesicles. The *pdr5*-deficient vesicles prepared from AD1−7 had no significant activity above background. Data illustrated in Figure 8B compare the ability of rhodamine 6G and tripentyltin chloride to inhibit IAAP cross-linking.

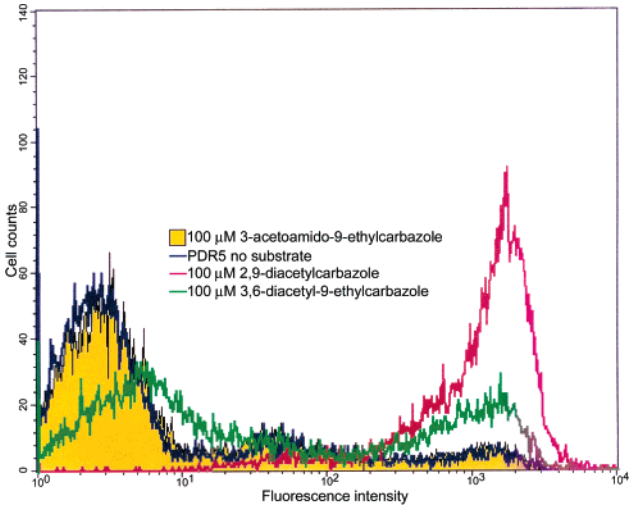

FIGURE 7: Inability of 3-acetoamido-9-ethylcarbazole to inhibit 2.5 μM rhodamine 6G efflux. Representative histogram plots for 100 μM 2,9-diacetylcarbazole, 3,6-diacetyl-9-ethylcarbazole, and 3-acetoamido-9-ethylcarbazole are shown. The plot of 3-acetoamido-9-ethylcarbazole indicates that there is no inhibition of rhodamine efflux when compared with the untreated control.

The former shows concentration-dependent inhibition. The latter is a potent Pdr5p substrate showing complete inhibition of [^{3}H]tritylimidazole efflux (*5*), yet it causes little or no inhibition of cross-linking. In fact, at lower concentrations, tripentyltin chloride seems to stimulate binding, although only one set of data points was obtained with this substrate. Thus, IAAP is site 1 specific.

Figure 8C shows a gel and representative phosphorimage demonstrating that clotrimazole shows concentration-dependent inhibition. Data from two independent experiments found in Figure 8D compare the ability of clotrimazole and tritylimidazole to inhibit cross-linking. While clotrimazole shows concentration-dependent inhibition, the effect of tritylimidazole is weak and saturating. An ANOVA statistical analysis was performed on the values used to construct Figure 8D. The probability that the samples are not different is <0.0001. Therefore, many observations made in whole cell transport assays are also seen at the level of direct Pdr5p−substrate interaction.

DISCUSSION

Although multidrug transporters are the subject of considerable study, most work focuses on the specificity of particular transporters to clinically important xenobiotic compounds that are chemically complicated. Thus, the specific chemical features used by multidrug binding sites to recognize substrates are not well understood. In this report, we use a novel approach to determine the substrate requirements of two Pdr5p binding sites that were initially defined by the ability to efflux chloramphenicol (site 1) and tritylimidazole (site 2). We used substrates that compose two series of structurally related derivatives. For the first time, we also determined that Pdr5p specifically binds IAAP at site 1. The conclusions reached with the binding assay and those obtained with whole cell transport studies are in excellent agreement. The data demonstrate that electronegative groups play a critical role in the specificity at both sites. At site 2, they function as hydrogen bond acceptor (electron pair donor) groups. At site 1, the data best support a model

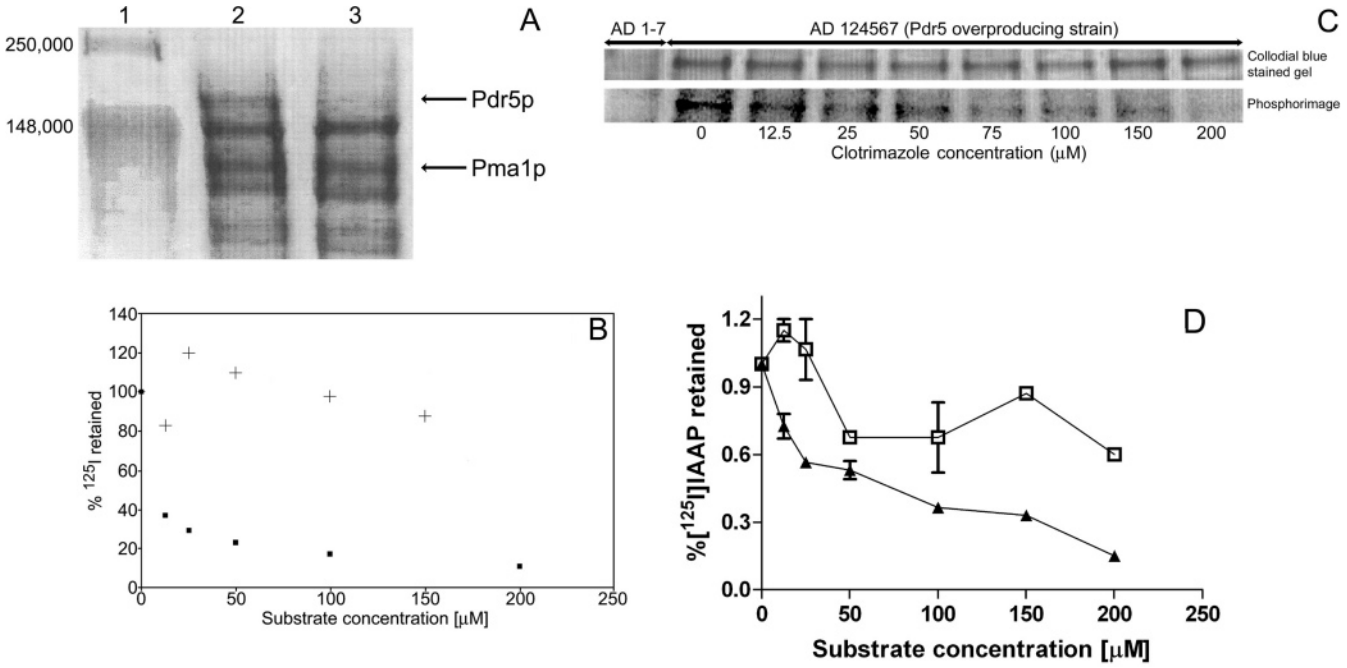

FIGURE 8: Inhibition of IAAP cross-linking by site 1 substrates. Photoaffinity labeling was carried out as described in the Experimental Procedures. (A) 15 μg of plasma membrane proteins solubilized in SDS−PAGE sample buffer and stained with Collodial Blue. Molecular mass markers (in daltons) are found in lane 1. The 160 kDa Pdr5p protein is overproduced in AD124567 (lane 2) and is absent in the *pdr5*Δ strain AD1−7 (lane 1), although the membrane ATPase Pma1p is present in both strains in equal quantity. The ratio of Pma1p to Pdr5p is ~1:1, an indication of high-quality membranes. (B) Plots for the effect of rhodamine 6G (■) and tripentyltin chloride (+) on IAAP binding. Because the data for each gel were obtained in different experiments, the intensity of the signal varies somewhat for each. Therefore, the value for the signal intensity from each data point is divided by that of the control sample for that particular experiment. (C) Collodial Blue-stained gel and phosphorimage of samples cross-linked with [^{125}I]IAAP in the presence of clotrimazole. (D) Comparative inhibition of IAAP cross-linking by tritylimidazole (□) and clotrimazole (▲). The data are the average of two separate experiments (four gels total) normalized as percent of the noncompeting substrate control because the signal varies somewhat for each gel. The actual arbitrary values for each point may be found through the supporting data link. The 200 μM clotrimazole concentration was used in only one experiment. Similarly, 150 μM tritylimidazole was used in one experiment and 200 μM in the other.

in which two groups in proximity are hydrogen bond acceptors, while a third group changes the electrostatic properties of an aromatic ring. Furthermore, analysis of two related carbazole derivatives suggests that the distances between these groups in site 1 may be critical for substrate−transporter affinity.

Previously (*5*), we showed that the site defined by tritylimidazole efflux (site 2) was used to efflux trialkyltin chlorides but not tetraalkyltins. This strongly suggested that at least one hydrogen bond acceptor group is required, because it is known that metallic halides are very good hydrogen bond acceptors (*13*). The present work reinforces this idea. Thus, trityl bromide, trityl ether, and methoxytrityl, which contain poor hydrogen bond acceptor groups, fail to exhibit concentration-dependent inhibition, unlike trityl derivatives with an alcohol or amine group. The alcohol and amine groups can also function as hydrogen bond donors as well as hydrogen bond acceptors. The fact that tritylimidazole contains only tertiary amines that are incapable of serving as hydrogen bond donors, as well as our observation that trialkyltin chlorides (*5*) cause complete inhibition of tritylimidazole efflux, argues that all of the groups function as hydrogen bond acceptors and that, under the conditions used, a proportion of the amine groups are unprotonated. Seelig (*14*) suggested that the π electrons of phenyl groups might serve as hydrogen bond acceptors during P-glycoprotein-mediated transport of xenobiotic molecules. This does not appear to be the case for substrates using Pdr5p site 2, because trityl derivatives such as trityl bromide, trityl ether, and methoxytrityl, which have three aromatic rings, do not show complete, concentration-dependent inhibition. Furthermore, Kolbe and Plass (*15*) demonstrated that aromatic tertiary amines are capable of forming hydrogen bonds. Therefore, hydrogen bonding involving the π electrons of phenyl groups in the carbazole derivatives is not necessary to explain the behavior of 9-butylcarbazole in the tritylimidazole efflux assay.

Three trityl and seven carbazole derivatives with two or more electronegative groups were used to explore substrate requirements at site 1 with a rhodamine efflux assay in whole cells and an IAAP cross-linking assay in purified plasma membrane vesicles. The results are striking. In each case, three electronegative groups are required for complete (or nearly complete) concentration-dependent inhibition. Two models are proposed to account for this observation. The first posits that all of the groups serve as electron pair donors (hydrogen bond acceptors). The second argues that two groups a short distance apart serve as donors, while the third influences the electrostatic properties of an aromatic ring, thus facilitating interaction with Pdr5p. At present, we favor the second model, for two reasons. First, while metallic halides are good hydrogen bond acceptors, chlorides attached to carbons are not (*13*). Second, all seven of the site 1 substrates, including chloramphenicol, IAAP, and rhodamine 6G, have a phenyl ring with a deactivating group. When a substrate (3-acetoamido-9-ethylcarbazole) is used that maintains the distances between electronegative groups but contains a ring-activating group rather than a deactivating

one, no site 1 inhibition is observed. The second model might also explain our previous observation that doxorubicin does not inhibit chloramphenicol efflux (*5*). This antitumor agent is known to be a Pdr5p substrate (*2*). Although doxorubicin has the requisite number and spacing of electronegative groups, those on the two aromatic rings are phenyl ring activators.

Further tests of these models are in progress. The work with 3-chloro-9-ethylcarbazole also suggests that if chlorine is acting to alter the electrostatic properties of the phenyl group, one deactivator group and one weak electron pair donor are not enough for concentration-dependent inhibition of rhodamine 6G. Thus, three groups appear to be necessary and at least two serve as hydrogen bond acceptors, depending on the model. Once it becomes clear which model is correct, the number and strength of acceptor groups can be evaluated better. It is important to note that the rhodamine 6G binding site of AcrB and QacR is structurally defined (*6*, *7*). In both proteins, hydrogen bond acceptor groups play a role in substrate−drug-binding protein interaction, although there appear to be significant differences. In the AcrB multidrug transporter, hydrophobic interactions seem to be predominant, although there appears to be a hydrogen bond between a lysine and the rhodamine ester group. The QacR site, however, contains multiple residues capable of hydrogen bonding that lie within 6 Å of the substrate. In this drug-binding protein, aromatic residues are also important. Electrostatic interactions between the rings in the substrates and those of binding site residues seem to play a significant role.

The behavior of 3,6-diacetyl-9-ethylcarbazole in efflux assays suggests that the distance between groups is important. Though this substrate has three electronegative groups, none of the distances are less than ~6.5 Å, and one is ~10 Å. In the FACS assay, 3,6-diacetyl-9-ethylcarbazole is a weaker inhibitor of rhodamine 6G efflux than is 2,9-diacetylcarbazole or NCC. Other explanations are of course possible. The two diacetyl derivatives have significant chemical differences. For instance, 3,6-diacetyl-9-ethylcarbazole has two strong electron-withdrawing groups (ring deactivators) on the rings, while 2,9-diacetylcarbazole has only one. Nevertheless, the three other substrates that we found to use site 1, IAAP, rhodamine 6G, and chloramphenicol, have at least one arrangement of three groups that resembles those found in the trityl and carbazole substrates showing complete inhibition [see Golin et al. (*5*) for inhibition of chloramphenicol efflux by clotrimazole].

In contrast, trityl and carbazole derivatives with two groups show a different behavior: partial inhibition exhibiting saturation at 15−30% of the fluorescence retained in the *pdr5* control. Similar saturating phenomena were observed by Kolaczkowski et al. (*2*) with Pdr5p and by others studying both bacterial and mammalian transporters (*7*, *16*, *17*). The explanation for such kinetics is that the partial inhibition or actual stimulation represents the binding of the interfering second substrate near, but not in the actual binding site of, the first. This behavior suggests that Pdr5p could have a binding pocket with overlapping and/or interacting binding sites.

Several other novel observations made in this study hint at structural overlap or proximity of sites 1 and 2. First, regardless of whether a substrate interacts at either site, the same MIC-size relationship is observed. For instance, clotrimazole and tritylimidazole are of similar surface volume and, within experimental error; exhibit the same MIC ratio, even though these xenophobic compounds interact at site 1 and site 2, respectively. This feature of Pdr5p substrates is consistent with the possibility that site 1 and site 2 overlap and/or that there is an optimal size requirement for entry into a common binding pocket. Alternatively, there could be multiple, nonoverlapping sites with similar size requirements. Second, although site 1 substrates such as clotrimazole also show complete inhibition of efflux from site 2 (*5*, as well as unpublished observations with site 1 substrates azidofluorescein diacetate, rhodamine 6G, and chloramphenicol), the converse is obviously not the case. Although other explanations are possible, this suggests that site 1 and site 2 could share a common hydrogen bond donor group(s) and that site 2 might be even be included in site 1.

In their landmark paper, Kolaczkowski et al. (*2*) introduced the rhodamine efflux assay as well as a transport assay measuring the quenching of rhodamine 6G fluorescence in plasma membrane preparations. This assay was used to test 22 substrates for the ability to inhibit rhodamine 6G quenching. Sixteen were classified as competitive inhibitors. We examined their structures to see if they exhibit the hydrogen bond acceptor, ring-deactivator pattern described above for site 1. Many of these are large, complex molecules with many electronegative groups. Nevertheless, of the 16, 11 substrates clearly have the requisite pattern and 3 certainly do not. The latter include tamoxifen, which contains two relatively weak hydrogen bond acceptors in proximity, and the steroid hormones progesterone and β-estradiol, each of which has two strong groups that are spaced in excess of 10 Å and no aromatic residue. Initially, we considered using steroid hormones instead of trityl derivatives to study specificity. However, we observed that in our whole cell rhodamine efflux assay, 50 μM progesterone caused a >50% increase in retained median fluorescence in the strain lacking Pdr5p (1727 arbitrary units untreated, 2713 with progesterone). Thus, these sterol derivatives could have a concentration-dependent, Pdr5p-independent effect that accounts for some of the differences between our results and those described above. Whether this can explain all of the differences between our respective data is not clear.

Our data confirm the presence of multiple Pdr5p−substrate binding sites and show that although two of the sites require hydrogen bond acceptor groups, the number at each site varies. Although our data suggest that aromatic groups may play an important role at site 1, at site 2 they are neither necessary nor sufficient. The novel use of several series of simple, chemically related substrates and the site-specific IAAP binding assay should prove to be useful in studying other multidrug transporters that are highly homologous to Pdr5p, such as the Cdr1p transporter found in the pathogen *Candida albicans*.

ACKNOWLEDGMENT

We thank Suneet Shukla for generously helping L.H. with the IAAP binding assay, Edwin Hanson and Robert Rutledge for patiently assisting with the graphics, and Trish Weisman for relentlessly editing the text. We had several important discussions with Dr. Kenneth Jacobson (NIH, NIDDK) on

the chemistry of imidazole and carbazole derivatives and greatly appreciate his contributions.

REFERENCES

1. Meyers, S., Schauer, W., Balzi, E., Wagner, M., Goffeau, A., and Golin, J. (1992) Interaction of the yeast pleiotropic drug resistance genes *PDR1* and *PDR5*, *Curr. Genet. 21*, 431−436.
2. Kolaczkowski, M., Vanderest, M., Cybularz-Kolaczkowski, A., Soumilluion, J., Konigs, W., and Goffeau, A. (1996) Anticancer drugs, ionophoric peptides and steroids as substrates of the yeast multidrug transporter Pdr5p, *J. Biol. Chem. 271*, 31543−31548.
3. Bissinger, P. H., and Kuchler, K. (1994) Molecular cloning of the *Saccharomyces cerevisiae STS1* gene product, *J. Biol. Chem. 269*, 4180−4186.
4. Golin, J., Barkatt, A., Cronin, S., Eng, G., and May, L. (2000) Chemical specificity of the *PDR5* multidrug resistance gene based on studies with tri-*n*-alkyltin chlorides, *Antimicrob. Agents Chemother. 44*, 134−138.
5. Golin, J., Ambudkar, S. V., Gottesman, M., Habib, A. D., Sczepanski, J., Ziccardi, W., and May, L. (2003) Studies with novel Pdr5p substrates demonstrate strong size dependence for xenobiotic efflux, *J. Biol. Chem. 278*, 5963−5969.
6. Yu, E., McDermott, G., Zgurskaya, H., Nikaido, H., and Koshland, D. (2003) Structural basis of multiple drug-binding capacity of the AcrB multidrug efflux pump, *Science 300*, 976−980.
7. Schumacher, M., Miller, M., and Brennan, R. (2004) Structural mechanism of simultaneous binding of two drugs to a multidrug-binding protein, *EMBO J. 23*, 2923−2930.
8. Rogers, B., Decottignies, A., Kolaczkowski, M., Caravajal, E., Moye-Rowley, W. S., and Goffeau, A. (2001) The pleiotropic drug ABC transporters from *Saccharomyces cerevisiae*, *J. Mol. Microbiol. Biotechnol. 3*, 207−214.
9. Shukla, S., Sani, P., Smirti, S., Iha, S., Ambudkar, S. V., and Prasad, R. (2003) Functional characterization of the *Candida albicans* ABC transporter Cdr1p, *Eukaryotic Cell 2*, 1361−1375.
10. Sauna, Z., and Ambudkar, S. V. (2001) Characterization of the catalytic cycle of ATP hydrolysis by human P-glycoprotein, *J. Biol. Chem. 276*, 11653−11661.
11. Leppert, G., McDevitt, R., Falco, S. V., Van Dyk, T. K., Ficke, M., and Golin, J. (1990) Cloning by gene amplification of two loci conferring multiple drug resistance in *Saccharomyces*, *Genetics 125*, 13−20.
12. Leonard, P., Rathod, P., and Golin, J. (1994) Loss-of-function mutation in the yeast multiple drug resistance gene *PDR5* causes a reduction in chloramphenicol efflux, *Antimicrob. Agents Chemother. 38*, 2492−2494.
13. Aullon, G., Bellamy, D., Brammer, L., Bruton, E. A., and Orpen, A. G. (1998) Metal-bound chlorine often accepts hydrogen bonds, *Chem. Commun.*, 653−654.
14. Seelig, A. (1998) A general pattern for substrate recognition by P-glycoprotein, *Eur. J. Biochem. 251*, 252−281.
15. Kolbe, A., and Plass, M. (2003) Heteroassociation of selected diols with some tertiary amines, *Z. Phys. Chem. 217*, 1411−1426.
16. Dey, S., Ramachandra, M., Pastan, I., Gottesmann, M. M., and Ambudkar, S. V. (1997) Evidence for two nonidentical drug interaction sites in the human P-glycoprotein, *Proc. Natl. Acad. Sci. U.S.A. 94*, 10594−10599.
17. Lewinson, O., and Bibi, E. (2001) Evidence for simultaneous binding of dissimilar substrates by the *Escherichia coli* multidrug transporter MdfA, *Biochemistry 40*, 12612−12618.

BI0502994